EPJ Web of Conferences **119**, 02004 (2016) DOI: 10.1051/epjconf/201611902004
ILRC 27

INJECTION SEEDED LASER FOR FORMALDEHYDE DIFFERENTIAL FLUORESCENCE LIDAR

G. Schwemmer [1]*, M. Yakshin[1], C. Prasad[1], T. Hanisco[2], A. R. Mylapore[3]†, I.H. Hwang[1], S. Lee[1]

[1]*Science & Engineering Services, LLC, Columbia, MD 21076, USA *Email: schwemmer@sesi-md.com*

[2]*NASA Goddard Space Flight Center, Greenbelt, MD 20771, USA*

[3]*MassTech, Inc., Columbia, MD 21076, USA*

†*currently with Aeromancer Technologies, Washington DC 20008, USA*

ABSTRACT

We describe the design and development of an injection seeded Nd:YVO_4 laser for use in a differential fluorescence lidar for measuring atmospheric formaldehyde profiles. A high repetition rate Q-switched laser is modified to accept injection seed input to spectrally narrow and tune the output. The third harmonic output is used to excite formaldehyde (HCHO) fluorescence when tuned to a HCHO absorption line. Spectral confirmation is made with the use of a photoacoustic cell and grating spectrometer.

1. INTRODUCTION

Formaldehyde (HCHO), both naturally occurring and anthropogenic, plays a key role in our understanding of short lived organic compounds in the atmospheric environment. It is a known carcinogen, respiratory irritant, and a component of smog. HCHO is a primary emission product of combustion and certain manufacturing processes, particularly for wood and paper products, but is also a degradation product of a large group of volatile organic compounds, both natural and man-made.[1] Hence, HCHO is an important target measurement for several environmental satellite programs, both existing and planned.[2]

In situ instruments can obtain precision measurements, but have limited coverage. An active in-situ sensor based on the Laser Induced Fluorescence (LIF) technique is the NASA In Situ Airborne Formaldehyde (ISAF) sensor[3], and is the foundation on which this instrument is based. Table 1 summarizes some of the current in situ instruments and techniques for formaldehyde measurements.

Besides the in-situ measurements, present remote sensing methods include long-term observations of HCHO columns from space using the Global Ozone Monitoring Experiment (GOME) satellite instrument launched in 1995.[7] GOME only provides column measurements and suffers from contaminations due to other atmospheric constituents such as O_3, NO_2, BrO and O_4. Other passive remote column measurement techniques include the Aura satellite's OMI instrument, ground-based FTIR and Multi-Axis Differential Optical Absorption Spectroscopy.[8]

Only the lidar can provide high vertical and spatial resolution simultaneously in a single instrument, making it a logical choice for HCHO science and satellite calibration and validation.

2. MEASUREMENT METHODOLOGY

HCHO fluoresces after exposure to ultraviolet (UV) radiation, appearing as a distinct series of spectral bands at specific wavelengths. The intensity of the fluorescence is proportional to the UV energy absorbed by the HCHO as well as its concentration. However, background fluorescence from other molecules and naturally occurring aerosols are also present in the same

Table 1. A comparison of some current in situ HCHO instruments and their levels of sensitivity.

Instrument	Techniques	Detection Limit (ppbv)	Time Resolution (s)
ISAF instrument[3]	LIF Technique	0.036	1
HCHO TDLAS[4]	TDLAS	0.05	2
Fourier Transform Infrared Interferometry White system – Chalmers University of Technology[5]	FTIR	0.4	5
Hantzsch AL4021 – Paul Scherrer Institute[6]	Fluorimetric Hantzsch Reaction	0.15	1.5

wavelength region. The HCHO fluorescence signal is maximized by tuning the UV transmitter to an HCHO absorption maximum (on-line). The laser is alternately switched between the on-line wavelength and an absorption minimum (off-line) in order to get a differential fluorescence measurement to remove unwanted background fluorescence from interfering gases and aerosols and determine the range resolved concentration of HCHO. A differential absorption lidar measurement can also be made from the elastic backscatter signals to get column content, but the very low concentration of HCHO makes its absorption too weak to resolve vertical structure.

The fluorescence emission spectrum of HCHO is shown in Figure 1.[9] Peaks in the spectrum correspond to vibronic transitions from the excited state to the ground state. The strongest is the 414 vibrational band located at 395.4 nm, indicated by the red line in Figure 1.

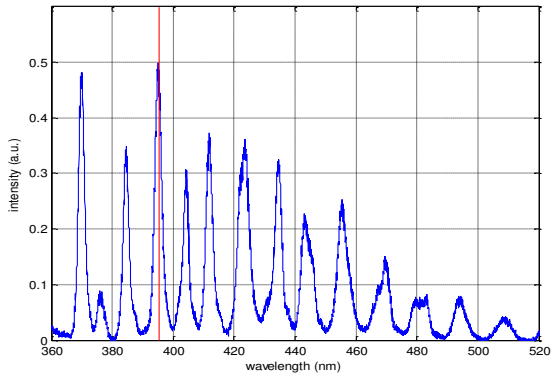

Figure 1. Fluorescence Spectrum of HCHO.

Rotationally resolved HCHO absorption measurements[10] have shown the presence of numerous strong lines in the 352 to 355 nm region, near the third harmonic wavelength of commonly used Nd:YAG and Nd:YVO_4 lasers. Figure 2 provides a plot of the portion of the HCHO absorption spectrum accessible to these lasers.

Table 2 shows the projected sensitivity of the instant lidar based upon our earlier results and the system parameters given below.[11, 12]

3. SYSTEM DESCRIPTION

We selected a diode pumped Coherent AVIA Nd:YVO_4 laser based on its reliability, high efficiency, and relatively broad (~ 0.15 nm) gain

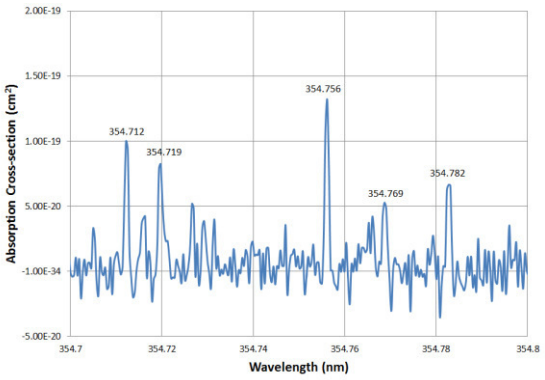

Figure 2. Rotationally resolved absorption spectrum for HCHO at 150 Torr, accessible to the third harmonic Nd:YVO_4 laser.

Table 2. Estimated sensitivity of the lidar.

Parameter	Value	
Integration Time	10 seconds	5 minutes
Range Resolution	1000 m	100 m
Sensitivity @ 1km	~85 ppt	~40 ppt

bandwidth as the starting point for the slave laser, modifying it to accommodate injection seeding. The use of a high rep-rate, low pulse energy limits this system to night time measurements only.

Figure 3 is a block diagram of the lidar system. It is configured as two assemblies, one containing a 30 cm diameter, 160 µrad field of view transceiver telescope, focal plane optics, and three photon counting photomultipliers to measure elastic backscatter, N_2 vibrational Raman backscatter, and the HCHO fluorescence signal. The fluorescence channel utilizes an interference filter produced specifically for HCHO measurements having 11-passbands between 380 and 480 nm that match the fluorescence bands shown in Figure 1. Further details of the system can be found in reference 12.

Referring again to Figure 3, the slave laser produces up to 1 W of UV Q-switched pulses at a 10 KHz rate. A narrow line (~1 MHz) single mode 1064 nm DFB diode laser is used to seed the slave laser through its output coupler. Four optical isolators (not shown) are used to prevent feedback. The slave laser head is mounted on a chill plate controlled by a small recirculating liquid chiller to maintain temperature stability.

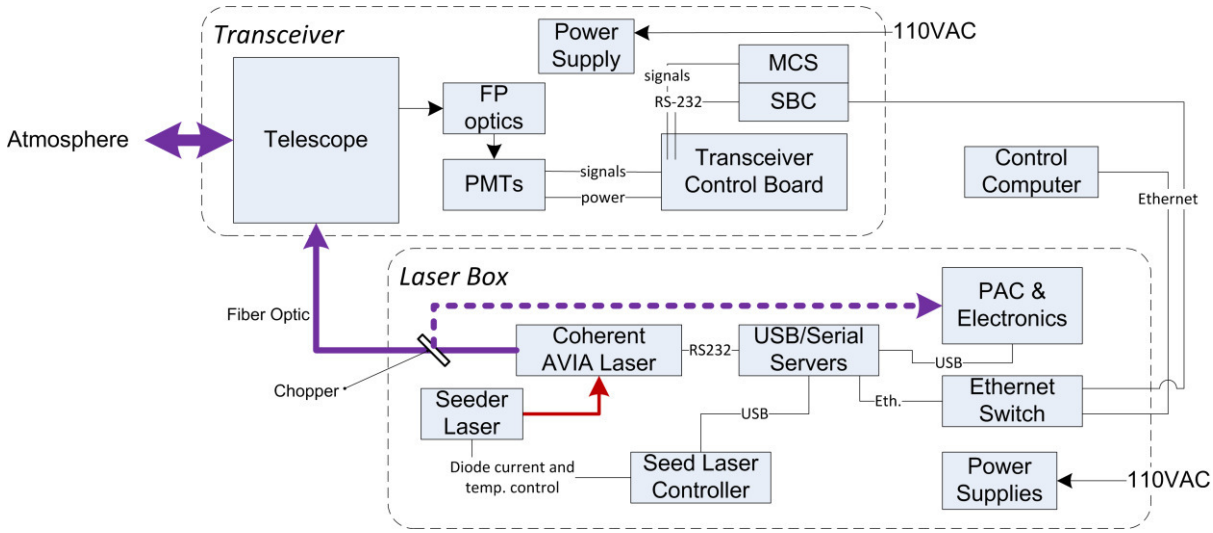

Figure 3. Block diagram of the HCHO lidar system.

4. INITIAL TEST RESULTS

A 46 Hz chopper equipped with a 4 mm wide mirror directs 0.35 ms bursts of laser pulses once per rotation to a photoacoustic spectroscopy (PAS) cell containing HCHO vapor. The PAS cell is resonant at 1.2 kHz and equipped with a microphone, whose signal is passed through a band pass amplifier centered at 1.2 kHz and digitized. We integrate the power in the PAS signal for 100 ms and normalize it by the laser power monitor signal to determine the magnitude of the absorption that takes place.

Continuous single mode seeded operation requires active control of the slave laser cavity length. However due to the monolithic nature of the construction of AVIA laser, it was not possible. Modulating the diode laser output to directly lock it to an HCHO UV absorption line is also not feasible since any rapid wavelength modulation is not conveyed to the slave laser's UV output when the cavity is not continuously seeded. Hence, we currently rely on the passive stability of the cavity to secure seeded operation. A 1-meter spectrometer equipped with a linear array detector (0.02 nm resolution in UV) is used to position the wavelength of the seed laser on or near the HCHO absorption line at 354.756 nm and also to determine the efficacy of injection seeding and its stability. When seeded, the output bandwidth shrinks from ~0.1 nm to ~0.02nm or less. The UV output power also drops significantly when the laser is well seeded, which may be due to spatial hole burning in the Nd:YVO_4 crystals when the laser is running single longitudinal mode.

Because the HCHO spectrum is fairly crowded with absorption lines, there is always a response by the PAS microphone when the laser is well seeded, partially seeded, or completely unseeded. In order to accurately locate on-line and off-line wavelengths, we perform scans of the seed laser wavelength across the gain bandwidth of the slave laser, by controlling the seed laser current. We monitor the PAS signal and the slave laser energy while also observing the spectrometer display to interpret the results. Figure 4 is a plot of the laser energy, the PAS signal amplitude, and laser power

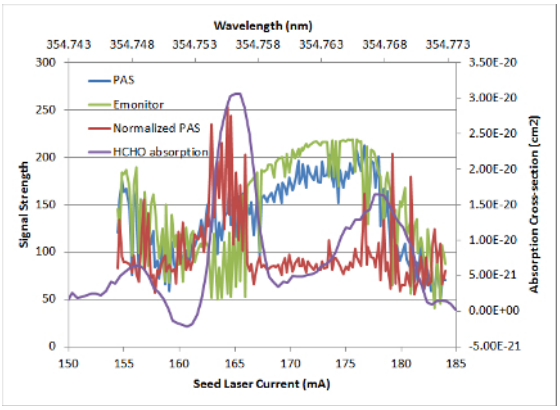

Figure 4. Current scan of the seed laser while plotting laser power (green) PAS signal power (blue), and PAS signal normalized for laser power (red). The absorption spectrum of HCHO is overlaid (violet).

normalized PAS amplitude as a function of the seed laser current. We have also overlaid a plot of the HCHO absorption cross section vs wavelength, where the correlation between diode current and wavelength was made using the spectrometer for a first order calibration and dispersion, then lining up the spectrum with features in the normalized PAS signal. Note the structure in the laser energy monitor signal (green line) across the scan as the slave laser goes in and out of seeded operation.

5. PATH FORWARD

Inconsistent seeding of the laser makes lidar data collection inefficient. This is because even when the seed laser wavelength is constant, drift in the slave laser cavity causes it to be unseeded for part of the time, and the fraction of corresponding data would need to be eliminated. Efforts are under way to achieve more stable seeded operation with the current system by improving the passive temperature stability and by using a broader line width seed laser that would overlap two to three slave cavity modes at any time, producing a multimode slave laser output that will stay seeded constantly, while still spectrally narrow with respect to the HCHO absorption line. Final integration and system level testing will follow.

ACKNOWLEDGEMENTS

We would like to acknowledge the engineering contributions of A. Achey, N. Mehta, and R. Clark of SES, and Dr. G. Li and K. Novoselov of MassTech, Inc. This work is supported by a MassTech purchase order under one of their SBIR contracts.

REFERENCES

[1] Abbot, D. S., et al., 2003: Seasonal and interannual variability of North American isoprene emissions as determined by formaldehyde column measurements from space, *Geophys. Res. Lett.,* **30 (7)**, 1886.

[2] NRC Decadal Survey 2007: Earth Science Applications from Space: National Imperatives for the next Decade and Beyond, National Research Council.

[3] M. Cazorla, *et al*., 2015: A new airborne laser-induced fluorescence instrument for in situ detection of formaldehyde throughout the troposphere and lower stratosphere, *Atmos. Meas. Tech*., **8**, 541-552.

[4] Wert, B. P., *et al*., 2003: Design and performance of a tunable diode laser absorption spectrometer for airborne formaldehyde measurements, *J. Geophys. Res*., **108**, 4350.

[5] Ritz, D., et al., 1993: An improved open-path multireflection cell for the measurement of NO2 and NO3, in: Optical methods in atmospheric chemistry, edited by: Schiff, H. I. and Platt, U., *SPIE Proceedings*, **1715**, 200–211.

[6] Kelly, T. J. and Fortune, C. R. 1994: Continuous monitoring of gaseous formaldehyde using an improved fluorescence approach, *Int. J. Environ. Anal. Chem.*, **54**, 249–263.

[7] Chance, K., *et al.,* 2000: Satellite observations of formaldehyde over North America from GOME, *Geophys. Res. Lett*., **27(21)**, 3461–3464.

[8] Jones, N., *et al.,* 2007: Long-term tropospheric formaldehyde concentrations deduced from ground-based Fourier transform solar infrared measurements, *Atmos. Chem. Phys. Discuss*., **7**, 14543-14568.

[9] Brackmann, C. *et al.,* 2003: Laser-induced fluorescence of formaldehyde in combustion using third harmonic Nd:YAG laser excitation, *Spectrochimica Acta Part A*, **59**, 3347

[10] Co, D. T., *et al.*, 2005: Rotationally resolved absorption cross sections of formaldehyde in the 28100-28500 cm^{-1} (351-356 nm) spectral region: Implications for in situ LIF measurements, *J. Phys. Chem. A,* **109(47)**, 10675 – 10682.

[11] Li, G., *et al*., 2012: Measurement of atmospheric formaldehyde profiles with a laser-induced fluorescence lidar, *Laser Radar Technology and Applications* XVII *Proc. SPIE,* **8379**, Paper 18.

[12] Mylapore, A. R., *et al*., 2014: Development of a fluorescence lidar for measurement of atmospheric formaldehyde, *Proc. SPIE,* **9080**, *Laser Radar Technology and Applications XIX; and Atmospheric Propagation XI*, 90800X (June 9, 2014); doi:10.1117/12.2053420.